Experimental and kinetic modeling study of oxidation of acetonitrile

Alzueta, María U.; Guerrero, Marta; Millera, Ángela; Marshall, Paul; Glarborg, Peter

Published in:
Proceedings of the Combustion Institute

Link to article, DOI:
10.1016/j.proci.2020.07.043

Publication date:
2021

Document Version
Peer reviewed version

Experimental and kinetic modeling study of oxidation of acetonitrile

Maria U. Alzueta,[1] Marta Guerrero,[1] Angela Millera,[1] Paul Marshall,[2] Peter Glarborg[3,*]

[1] Aragon Institute of Engineering Research I3A, Department of Chemical and Environmental Engineering, University of Zaragoza, 50018 Zaragoza, Spain

[2] Department of Chemistry and Center for Advanced Scientific Computing and Modeling, University of North Texas, 1155 Union Circle #305070, Denton, Texas 76203-5017

[3] DTU Chemical Engineering, Technical University of Denmark, DK-2800 Lyngby, Denmark

[*] Corresponding author: pgl@kt.dtu.dk

Preferred colloquium: *Gas-Phase Reaction*

Total length of paper (without abstract): 5546 words

Method of determination: Method 1

Equivalent lengths:

- Main text: 2763 words
- References (50+2)x2.2x7.7: 881 words
- Tables (2): (29+2)x7.6x2 + (7+2)x7.6x2 = 608 words
- Figures: 1294 words
  - Fig. 1: (47+10)×2.2 and 48 words in caption→ 173 words
  - Fig. 2: (55+10)×2.2 and 43 words in caption→ 186 words
  - Fig. 3: (116+10)×2.2 and 10 words in caption→ 287 words
  - Fig. 4: (52+10)×2.2 and 24 words in caption→ 160 words
  - Fig. 5: (33+10)×2.2 and 45 words in caption→ 140 words
  - Fig. 6: (44+10)×2.2 and 70 words in caption→ 189 words
  - Fig. 7: (56+10)×2.2 and 14 words in caption→ 159 words

Supplemental material available

Experimental and kinetic modeling study of oxidation of acetonitrile

María U. Alzueta[a], Marta Guerrero[a], Ángela Millera[a], Paul Marshall[b], Peter Glarborg[c]

[a] *Aragón Institute of Engineering Research I3A, Department of Chemical and Environmental Engineering, University of Zaragoza, 50018 Zaragoza, Spain*
[b] *Department of Chemistry and Center for Advanced Scientific Computing and Modeling, University of North Texas, 1155 Union Circle #305070, Denton, Texas 76203-5017*
[c] *DTU Chemical Engineering, Technical University of Denmark, DK-2800 Lyngby, Denmark*

Abstract

Oxidation of acetonitrile has been studied in a flow reactor in the absence and presence of nitric oxide. The experiments were conducted at atmospheric pressure in the temperature range 1150-1450 K, varying the excess air ratio from slightly fuel-lean to very lean. Oxidation of CH_3CN was slow below 1300 K. Nitric oxide, hydrogen cyanide and nitrous oxide were detected as important products. A detailed chemical kinetic model for oxidation of acetonitrile was developed, based on a critical evaluation of data from literature. The rate coefficients for the reactions of CH_3CN and CH_2CN with O_2 were calculated from ab initio theory. Modeling predictions were in satisfactory agreement with experiments. Calculations were sensitive to thermal dissociation of CH_3CN and to the branching fraction for CH_3CN + OH to CH_2CN + H_2O and HOCN + CH_3, respectively. More work is desirable for these steps, as well as for reactions of CH_2CN and HCCN.

Keywords:

CH_3CN oxidation, flow reactor experiments, ab initio theory, kinetic modeling

Introduction

Nitriles are potentially important fuel-nitrogen intermediates in the combustion of solid fuels. They may be formed from the decomposition of different nitrogen functionalities [1–3] and acetonitrile has been observed in coal pyrolysis gases [4]. Nitriles may also be formed from fuel-cyanide interactions under locally reducing conditions [5, 6]. The high temperature pyrolysis and oxidation of a number of nitriles have been studied, i.e., acetonitrile [7–14], acrylonitrile [8, 10], and benzonitrile [8, 15–17].

Acetonitrile (CH_3CN) is the simplest of the nitriles, but knowledge of its chemistry is limited compared to that of other reactive nitrogen species, such as HCN and NH_3. Acetonitrile has been proposed as an important nitrogen intermediate in oxidation of CH_4/NH_3 mixtures in a flow reactor [18], where it can be formed by the reaction CH_3 + HCN $\rightarrow$ CH_3CN + H (R4b). This reaction serves to recycle the nitrogen between cyanide species, but it is not known to what extent the formation of CH_3CN affects the selectivity for forming NO or N_2. In the past, these recycle reactions have been assumed to be of minor significance for modeling predictions of nitrogen chemistry [5]. It is believed that, at least in high temperature flames, the form of reactive nitrogen has only a minor influence on the selectivity for forming NO [6]. This assumption is supported by the results of Williams and Fleming [19], who report that NH_3, CH_3NH_2, and CH_3CN doped to a stoichiometric, low-pressure CH_4/O_2/Ar flame yield similar amounts of NO. However, due to

the scarcity of experimental results and the uncertainties in the reaction mechanism of even the simplest nitriles, this is presently difficult to verify.

Previous studies of CH_3CN cover both pyrolysis and oxidation. The pyrolysis work was performed in flow reactors [7, 8] and in shock tubes [9, 10, 13, 14], while reported studies on ignition and oxidation were conducted in shock tubes [11, 12]. In addition, Kramlich et al. [20] investigated its selectivity for forming N_2O in a flow reactor. Oxidation mechanisms for oxidation of CH_3CN have been proposed by Ikeda and Mackie [11], Lifshitz et al. [12], and Williams and Fleming [19].

The objective of the present study is to establish and validate a detailed chemical kinetic model for oxidation of CH_3CN, based on our present knowledge of nitrogen chemistry. Atmospheric pressure flow reactor experiments are conducted over a range of temperature and stoichiometry, with and without the presence of NO. The modeling work is based on the recent review of Glarborg et al. [21], revising the reaction subset for CH_3CN drawing on theory as well as recent experimental work. The reactions of CH_3CN and CH_2CN with O_2 are characterized by ab initio theory. The flow reactor experiments are interpreted in terms of the kinetic model and the important reactions in the oxidation are identified.

Experimental

The experiments were carried out at atmospheric pressure in a quartz tubular flow reactor used previously for studying gas-phase hydrocarbon and nitrogen chemistry at high temperature (see for instance [5, 22–24]). It is based on the design developed by Kristensen et al. [25]. The quartz reactor

had an isothermal reaction zone of 20 cm in length and an internal diameter of 0.87 cm. The total flow rate in all experiments was 1 L min^{-1} (STP), resulting in a gas residence time being a function of temperature. The reactor was placed in a three-zone electrically heated oven, ensuring a uniform temperature profile (±5 K) along the reaction zone.

Reactant gases from cylinders (CH_3CN, O_2, NO, and N_2) were led to the reactor in up to four separate streams, following the procedure of Alzueta et al. [22]. The gas cylinders contained high purity gases with a maximum relative uncertainty of 2%, determined for a confidence interval of 95%. Water vapor was fed by saturating a nitrogen stream through a bubbling water system at room temperature. The mass flow controllers (Brooks) had a maximum error of 1.5%. The gases were mixed just prior to the reactor inlet. At the outlet of the reaction zone, the product gas was cooled by means of external refrigeration with air. The exhaust gases passed through a condenser and a filter, and were subsequently lead to the analysis system, which included a UV continuous analyzer for NO, an IR continuous analyzer for CO and CO_2, and an FTIR spectrometer (e.g., CH_3CN, CH_4, HCN, and N_2O). Other possible products, such as C_2H_6, NH_3, HNCO, and NO_2, could also be detected by FTIR, but were present only in negligible amounts. The accuracy of the measurements was estimated to be within 5%.

Detailed Kinetic Model

The starting mechanism and corresponding thermodynamic properties were drawn from the recent review on nitrogen chemistry by Glarborg et al. [21]. The thermodynamic properties for species in the acetonitrile subset were

largely drawn from the Burcat database [26]. The full reaction mechanism including thermodynamic data is available as Supplemental Material (SM). Table 1 lists the key reactions in the CH_3CN oxidation subset with the rate coefficients used in the present work. Only reactions in the acetonitrile subset of the mechanism were updated, compared to the kinetic model of Glarborg et al. [21].

The thermal dissociation of CH_3CN mainly proceeds through H elimination, $CH_3CN(+M) \rightleftharpoons CH_2CN + H\ (+M)$ (R1b), while C–C bond fission to form $CH_3 + CN$ (R2) is less important due to the strong C-C bond. No direct measurements are available, but values of k_{1b} in the fall-off region have been derived from shock tube pyrolysis and oxidation experiments [11, 12, 14]. The interpretation of the shock tube results is affected by secondary chemistry, which is not well established, and there is significant scatter in the reported results. In the present work, we rely on the results by Sendt et al. [14]. We have adopted their calculated value of the high pressure limit $k_{1b,\infty}$ and, based on unimolecular rate theory [35, 36], estimated a low pressure limit $k_{1b,0}$ from their reported data in the fall-off region (12 atm) and an assumed center broadening fractor F_c of 0.49 to arrive at the rate coefficients shown in Table 1.

Reactions of CH_3CN with the radical pool typically have two major product channels, forming CH_3 or abstracting H to form CH_2CN. Under the present conditions, OH is the main chain carrier. The mechanism of the CH_3CN + OH reaction has been in discussion. Low temperature studies [37, 38] supported by theory [39] indicate that H-abstraction (R8) and formation of a $CH_3C(OH)N$ adduct accounts for roughly 50% each of the reac-

		A	β	E_a	Source
1.	$CH_3CN(+M) \rightleftharpoons CH_2CN + H(+M)$	9.2E12	0.850	95770	[14], see text
	Low pressure limit (Ar)	2.9E19	0.000	94850	
	$F_c = 0.49$, $N_2 = 1.5$				
2.	$CH_3CN \rightleftharpoons CH_3 + CN$	1.0E15	0.000	117000	[14] est
3.	$CH_3CN + H \rightleftharpoons CH_2CN + H_2$	6.0E04	3.010	8522	[27]
4.	$CH_3CN + H \rightleftharpoons CH_3 + HCN$	4.4E10	0.800	6800	[27]
5.	$CH_3CN + H \rightleftharpoons CH_3 + HNC$	2.8E15	-0.320	20030	[27]
6.	$CH_3CN + O \rightleftharpoons CH_2CN + OH$	4.7E08	1.180	14360	[28]
7.	$CH_3CN + O \rightleftharpoons CH_3 + NCO$	6.0E09	1.180	8130	[28]
8.	$CH_3CN + OH \rightleftharpoons CH_2CN + H_2O$	2.7E02	3.270	494	[29]
9.	$CH_3 + HOCN \rightleftharpoons CH_3CN + OH$	5.0E12	0.000	2000	[5] est
10.	$CH_3CN + O_2 \rightleftharpoons CH_2CN + HO_2$	2.4E15	0.000	58000	pw (1250-3000 K)
11.	$CH_3CN + CH_3 \rightleftharpoons CH_2CN + CH_4$	5.0E12	0.000	7000	[14]
12.	$CH_3CN + CN \rightleftharpoons CH_2CN + HCN$	1.6E13	0.000	2430	[30], fit, >700 K
13.	$CH_2CN + H \rightleftharpoons HCCN + H_2$	1.2E06	2.430	6000	est CH_3+H
14.	$CH_3 + CN \rightleftharpoons CH_2CN + H$	1.0E14	0.000	0	[5] est
15.	$CH_2CN + O \rightleftharpoons CN + CH_2O$	1.0E12	0.640	0	[31], est
16.	$CH_2CN + O \rightleftharpoons OCHCN + H$	3.0E11	0.640	0	[31], est
17.	$CH_2CN + OH \rightleftharpoons HCCN + H_2O$	4.3E04	2.568	3997	est CH_3+OH
18.	$CH_2CN + O_2 \rightleftharpoons OCHCN + OH$	2.5E12	0.000	29700	pw (1250-3000 K)
19.	$CH_2CN + O_2 \rightleftharpoons OCH_2CN + O$	2.5E12	0.000	38700	pw
20.	$CH_2CN + CH_2CN \rightleftharpoons NCCH_2CH_2CN$	2.3E13	0.000	0	[14]
21.	$HCCN + O_2 \rightleftharpoons HCN + CO_2$	1.1E12	0.000	0	[32]
22.	$HCCN + NO \rightleftharpoons HCN + NCO$	2.1E13	0.000	0	[32]
23.	$OCHCN \rightleftharpoons HCN + CO$	3.5E14	0.000	66300	[33] (k_∞)
24.	$OCHCN \rightleftharpoons HNC + CO$	1.1E15	0.000	65300	[33] (k_∞)
25.	$OCHCN + OH \rightleftharpoons NCCO + H_2O$	2.4E07	1.830	-1116	est CH_2O+OH
26.	$NCCO + O_2 \rightleftharpoons NCO + CO_2$	7.0E10	0.000	0	[34]

Table 1: Reaction subset for acetonitrile oxidation. Parameters for use in the modified Arrhenius expression $k = AT^{\beta} \exp(-E/[RT])$. Units are cm, mol, s and cal.

tion. For the H-abstraction channel (R8), we use the calculated rate constant from Li and Wang [29], which is in reasonable agreement with the low temperature measurements [37, 40–42]. At elevated temperatures, the adduct is not expected to be stable. However, the present results, discussed below, support a product channel forming methyl, CH_3 + HOCN (R9b). There are no reported measurements for this reaction. We have adopted the rate constant estimated by Miller [5]. The branching fraction of the CH_3CN + OH reaction has a significant influence on modeling and more work on this step is desirable.

For CH_3CN + H (R3, R4), we have adopted the calculated rate constants from Wang et al. [27]; they agree roughly within a factor of two with the early measurements in the 313-780 K range by Jamieson et al. [43]. The overall rate constant for CH_3CN + O was measured directly at low temperatures by Bonnano et al. [44]; their results are in good agreement with the recent theoretical study of Sun et al. [28]. Formation of CH_3 + NCO (R7) is predicted to be the major product channel in the 800-1500 K range, while direct H-abstraction (R6) becomes important above 1500 K.

Other reactions of CH_3CN include H-abstraction by O_2 (R10), CH_3 (R11), and CN (R12). There are no direct measurements for last two of these reactions, but values of k_{11} and k_{12} are available from an indirect shock tube determination [14] and theory [30], respectively. In the present work, we analyzed the CH_3CN + O_2 reaction from ab initio theory. Geometries of the reactants and the transition state for H-atom abstraction were obtained through application of M06-2X/6-311+G(2df,2p) density functional theory [45]. The results are given in SM. Harmonic vibrational frequencies were

obtained and scaled by factors of 0.971, for zero-point energy, and 0.946, for fundamental frequencies to determine vibrational partition functions [46]. Then single-point energies were derived via the CBS-APNO methodology, which approximates extrapolation of coupled cluster results to the complete basis set limit [47]. For difficult nitrogen species like N-oxides and CN with high spin-contamination, data in ref. [47] for species with similarity to those met here yield NO, CN and NH_2 atomization energies with errors of -0.6, +0.4 and +0.1 kcal/mol, respectively. Our method yields the H-CH_2CN bond strength to within 0.5 kcal/mol of the ATcT value [48]. Similar accuracy has been obtained in other work of ours for CH_xN_y (x=0-3, y=0-2) C-H and N-H bond strengths [49]. A conservative uncertainty for our computed reaction enthalpies and barriers is ca. 1 kcal/mol. Calculations were made with the Gaussian 16 program [50]. They yielded a 0 K reaction barrier of 48.6 kcal mol^{-1}. A one-dimensional Eckart model for tunneling and a hindered rotor treatment, based on a relaxed scan of the rotational potential for the O_2 molecule spinning around the nascent O-H bond, were incorporated into the transition state theory evaluation via the Multiwell-2019 program suite [51]. The analysis yielded a rate constant of k_{10} = 2.4E15 exp(-29200/T) cm^3 mol^{-1} s^{-1} for 1250-3000 K.

There are only limited data available for reactions of CH_2CN. Hoyermann et al. [31] characterized CH_2CN + O experimentally, finding it to be very fast. They detected formation of formyl cyanide (OCHCN), formaldehyde, and an OCH_2CN adduct, but could not quantify branching fractions. We tentatively assume CH_2O + CN (R15) to be the major channel, with a smaller contribution from OCHCN + H (R16). Reactions of CH_2CN with H and OH

yield primarily HCCN (R13, R17); the rate constants were estimated by analogy with CH_3 reactions.

Similarly to the methyl radical, cyanomethyl (CH_2CN) is not very reactive towards O_2. Addition of O_2 to form a peroxy radical is slow, even at room temperature [52]. In the absence of data at elevated temperature, we studied the reaction theoretically by the same methods outlined above for $CH_3CN + O_2$. The results are summarized in the potential energy diagram of Fig. 1. The reaction involves initial formation of $OOCH_2CN$, which is quite strongly bonded, with OO–CH_2CN = 19.4 kcal mol^{-1}. At high temperatures, the peroxy will not be stable, however, and chemistry will proceed via well-skipping. The most energetically favorable dissociation path is isomerization of the peroxy to HOOCHCN, which in turn is unstable with respect to dissociation to OH + OCHCN, formyl cyanide. The bottle neck is the isomerization with a barrier of 22.7 kcal mol^{-1} relative to O_2 + CH_2CN. Our computed rate constant for O_2 + $CH_2CN \rightarrow$ OH + OCHCN (R18) is 2.5E12 exp(-7100/T) cm^3 mol^{-1} s^{-1} for 1250-3000 K. Extrapolation of k_{18} to lower temperatures would be quite uncertain because of tunneling effects, but similarly to $CH_3CN + O_2$ (R10), $CH_2CN + O_2$ is too slow below 1250 K to play a role. Dissociation of $OOCH_2CN$ to O + OCH_2CN has no barrier beyond the endothermicity of 38.7 kcal mol^{-1} relative to O_2 + CH_2CN. We take this value as a rough estimate of E_a, along with an assumed A-factor for k_{19}.

The HCCN radical is mainly consumed by the fast reaction with O_2. This step was studied experimentally by Adamson et al. [32] at low temperature. They observed HCN, HNC and CO_2 among the products, but could not

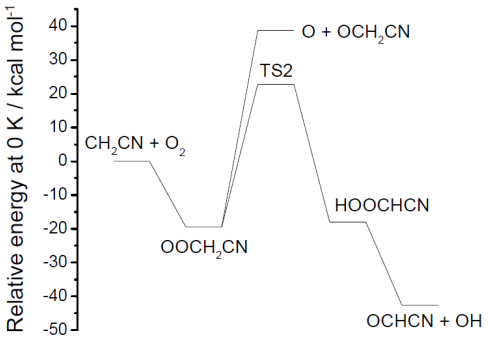

Figure 1: Potential energy surface for the $CH_2CN + O_2$ reaction.

detect any CHNO isomers. Wang et al. [53] studied the reaction theoretically, identifying the most probable product channels to be HCN + CO_2, HNC + CO_2, and HNCO + CO; all proceeding without a barrier. Following the observations of Adamson et al. [32], we assume the products of reaction to be HCN + CO_2 (R21). Under the conditions of the present study, any HNC formed from HCCN + O_2 will rapidly isomerize to HCN.

The $CH_2CN + O_2$ reaction forms primarily formyl cyanide, OCHCN (R18). The small amount of OCH_2CN formed (R19) is assumed to form OCHCN by dissociation or reaction with O_2. Dissociation of OCHCN to form CO + HCN and CO + HNC has been studied theoretically [33]. Rate constants for reactions of OCHCN with the radical pool, the most important being OCHCN + OH $\rightarrow$ NCCO + H_2O (R25), were estimated by analogy to formaldehyde reactions. Most likely, the NCCO formed reacts mainly with O_2. This step has been investigated at low temperature by Imamura and Washida [54] and Feng and Hershberger [55] and their results are in good agreement. The reaction is pressure dependent at low temperature, forming

mainly a peroxide adduct, but a minor channel yields NCO + CO_2 (R26). Presumably, R26 is the only important channel at high temperatures; we have derived a value for k_{26} from the theoretical work of Wang et al. [34]. The reaction of NCCO with NO forms an adduct at low temperatures [56] and is not likely to be important under the present conditions.

Results and Discussion

The flow reactor experiments on CH_3CN oxidation were conducted with and without addition of NO, varying temperature in the range 1150-1450 K and excess air ratio λ between 1.7 and 31. The experimental conditions are summarized in Table 2. Water vapor was added to the experiments to provide a reactant composition resembling better a real flue gas and to reduce any potential surface activity on the reactor wall. The addition of NO in selected experiments was useful to provide further information about the CH_3CN oxidation mechanism. Due to the fast reaction NO + $HO_2 \rightleftarrows$ NO_2 + OH, the NO/NO_2 ratio is a measure of the importance of HO_2 in the oxidation. Furthermore, the consumption of NO and formation of products provide information on reactive N-intermediates. Below, we only show results for sets 1, 2, 5, and 6. Data sets 3 and 4 are quite similar to those of sets 1 and 2, respectively. Experimental data in tabular format for all experiments can be found in SM. The carbon balance in the experiments closed within 4%.

Figure 2 compares experimental data for CH_3CN oxidation at slightly lean conditions with modeling predictions. The calculations were conducted with Chemkin PRO [57]. Consumption of acetonitrile proceeds very slowly

Exp.	CH_3CN (ppm)	O_2 (ppm)	NO (ppm)	H_2O (%)	λ	τ (s)
1	157	862	-	2.1	1.67	200/T(K)
2	157	864	820	2.1	1.69	200/T(K)
3	157	1082	-	1.5	2.14	200/T(K)
4	157	1084	824	1.5	2.11	200/T(K)
5	160	15652	-	1.8	30.10	198/T(K)
6	158	15731	819	1.8	30.63	195/T(K)

Table 2: Conditions for the flow reactor experiments. λ is the excess air ratio and τ is the residence time in the isothermal zone of the reactor.

at temperatures below 1350 K. Above 1350 K the decay is faster, but even at 1450 K only of the order of 50% of the inlet CH_3CN is consumed. Oxidation of CH_3CN leads to formation of CO, HCN, and CH_4, while concentrations of CO_2, NO, N_2O, and HNCO are small or below the detection limit of a few ppm. The kinetic model captures the low reactivity of acetonitrile, predicting correctly onset of reaction above 1350 K. However, the decomposition of CH_3CN is underpredicted at the highest temperatures, resulting in underprediction of the products, in particular CO and HCN. Considering the uncertainties in the reaction mechanism, in particular the rate constant for CH_3CN dissociation (R1) and the branching fraction for CH_3CN + OH (R8, R9), we consider the agreement to be satisfactory.

Figure 3 shows the effect of adding NO to the inlet under conditions similar to those of Fig. 2. Comparison of the two figures shows that presence of NO has only a minor impact on the process. Nitric oxide does not promote oxidation of CH_3CN and no oxidation of NO to NO_2 is observed. This shows that formation of HO_2 by H-abstraction by O_2 from CH_3CN or CH_2CN is

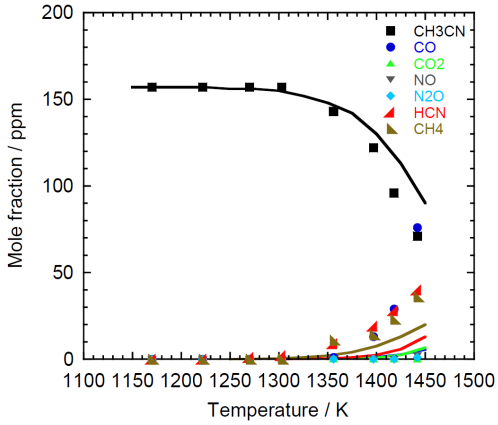

Figure 2: Comparison of experimental and predicted mole fractions for oxidation of CH_3CN in a flow reactor under slightly lean conditions (λ = 1.67, set 1). The symbols mark experimental data while solid lines denote model predictions. Conditions: P = 1.05 atm, residence time τ(s) = 200 / T(K); inlet composition is 157 ppm CH_3CN, 862 ppm O_2, 2.1% H_2O; balance N_2.

unimportant, in agreement with the theoretical work on these two steps; peroxides play no role in the oxidation of CH_3CN. Hydrogen cyanide and methane are formed in levels similar to those in the absence of NO, while CO formation is suppressed. Only at temperatures above 1400 K, NO is consumed and only to a small extent. The absence of N_2O formation indicates that formation of the NCO radical is very limited under these conditions. The modeling predictions are in satisfactory agreement with measurements, except for underpredictions of CO and HCN.

Figure 4 shows results for CH_3CN oxidation under very lean conditions. The larger excess of O_2 promotes oxidation of acetonitrile, which now is initiated below 1300 K. Between 1300 and 1400 K, concentrations of the intermediates CO, HCN, and CH_4 peak. Above 1400 K, all CH_3CN is oxidized

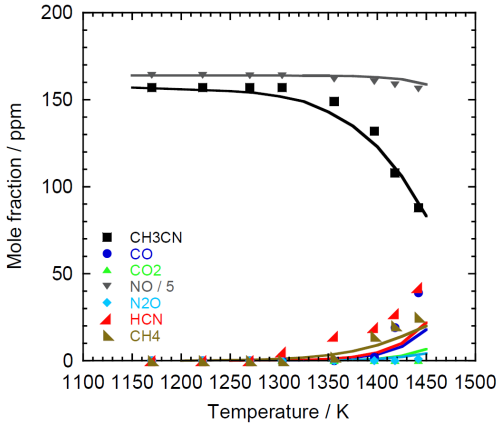

Figure 3: Comparison of experimental and predicted mole fractions for oxidation of CH_3CN in a flow reactor under slightly lean conditions in the presence of NO ($\lambda = 1.69$, set 2). The symbols mark experimental data while solid lines denote model predictions. Conditions: P = 1.05 atm, residence time τ(s) = 200 / T(K); inlet composition is 157 ppm CH_3CN, 864 ppm O_2, 820 ppm NO, 2.1% H_2O; balance N_2.

to CO_2, along with significant amounts of NO. Also N_2O is now detected, peaking with 30 ppm at 1400 K. The modeling predictions are in good agreement with measurements, with the formation of NO captured quantitatively. However, N_2O is underpredicted by about a factor of two.

Figure 5 shows the effect of adding NO under very lean conditions. Similar to observations for the near-stoichiometric case, presence of NO has little impact on the CH_3CN consumption. Also, peak concentrations of CO, HCN, and CH_4 are largely unaffected. The main change is a larger peak level for N_2O, coinciding with a reduction in NO considerably larger than at near-stoichiometric conditions. This is captured by the modeling predictions, which are in good agreement with measurements. The formation of N_2O, promoted by the presence of NO, indicates that NCO is formed during

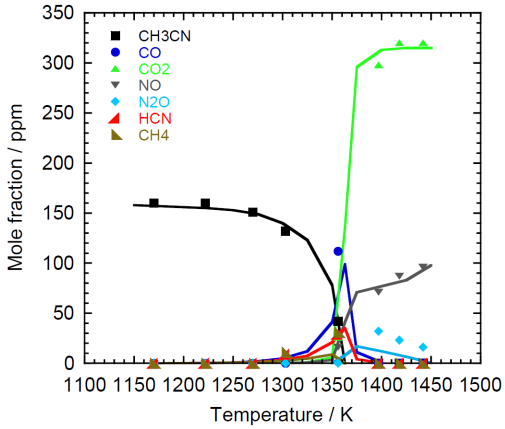

Figure 4: Comparison of experimental and predicted mole fractions for oxidation of CH_3CN in a flow reactor under very lean conditions (λ = 30.1, set 5). The symbols mark experimental data while solid lines denote model predictions. Conditions: P = 1.05 atm, residence time τ(s) = 198 / T(K); inlet composition is 158 ppm CH_3CN, 1.57% O_2, 1.8% H_2O; balance N_2.

oxidation; N_2O is formed by the fast reaction of NCO with NO.

Figure 6 shows a simplified reaction pathway diagram for oxidation of CH_3CN under the investigated conditions. Acetonitrile is largely consumed by thermal dissociation (R1b) or reaction with OH (R8, R9b). The relative importance of these consumption pathways varies strongly with stoichiometry and temperature. Two major oxidation paths can be identified; one going through CH_2CN (R1b, R8) and one via CH_3 and HOCN (R9b). The path through CH_2CN leads mainly to HCN via the reaction sequences $CH_2CN \xrightarrow{+OH} HCCN \xrightarrow{+O_2} HCN$ and $CH_2CN \xrightarrow{+O} CN \xrightarrow{+H_2O} HCN$. Both these sequences are chain terminating, causing the acetonitrile oxidation to proceed only at high temperatures. The pathway through HOCN yields NCO, which then reacts with NO, H_2O, or atomic O to form a range of N-species; HNCO, NO,

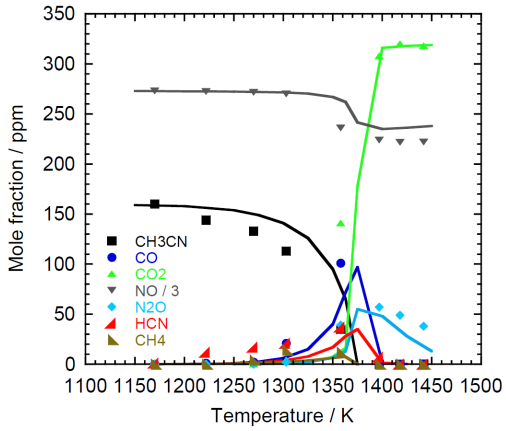

Figure 5: Comparison of experimental and predicted mole fractions for oxidation of CH_3CN in a flow reactor under very lean conditions in the presence of NO (λ = 30.6, set 6). The symbols mark experimental data while solid lines denote model predictions. Conditions: P = 1.05 atm, residence time τ(s) = 198 / T(K); inlet composition is 160 ppm CH_3CN, 1.57% O_2, 819 ppm NO, 1.8% H_2O; balance N_2.

N_2O, or N_2. While these steps are mostly chain terminating, formation of the methyl radical from CH_3CN + OH (R9b) leads to a sequence of reactions that replenish the radical pool and promote oxidation. A minor pathway not shown in Fig. 6 involves the sequence $CH_2CN \xrightarrow{+O}$ ($OCH_2CN \xrightarrow{+M,O_2}$) OCHCN $\xrightarrow{+OH}$ NCCO $\xrightarrow{+O_2}$ NCO. It should be noted that according to the present model, pathways through HCCN and NCCO both lead to formation of CO_2, which was not observed as an important product in the experiments.

Figure 7 shows a sensitivity analysis for CH_3CN for the conditions of Figs. 2 and 4. The reaction with the largest sensitivity coefficients is the thermal dissociation of CH_3CN (R1b), which strongly promotes reaction. The branching fraction of CH_3CN + OH is important, with formation of CH_3 + HOCN (R9b) generating chain carriers, while the channel to CH_2CN

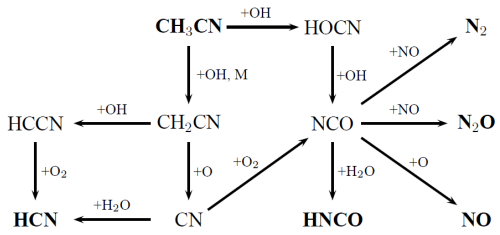

Figure 6: Simplified reaction path diagram for oxidation of CH_3CN under lean conditions.

(R8) initiates a chain terminating sequence. Also the reactions of O_2 with CH_3CN (an initiation step) and CH_2CN serve to promote oxidation under very lean conditions.

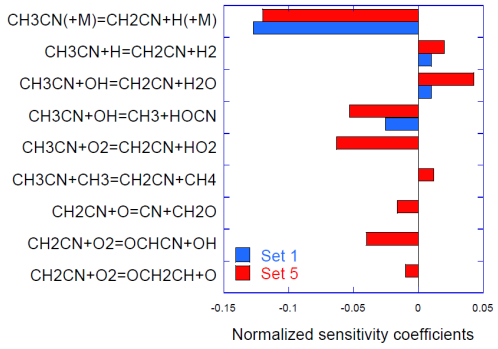

Figure 7: First-order sensitivity of the predicted CH_3CN concentration for the conditions of set 1 (1350 K) and set 5 (1300 K).

Conclusions

Oxidation of acetonitrile has been studied in a flow reactor in the absence and presence of nitric oxide. The experiments, conducted at temperatures of 1150-1450 K, show that CH_3CN oxidation is controlled by chain terminating reaction sequences, resulting in slow reaction below 1300 K. Major oxidation products included NO, HCN and N_2O, while HNCO was not detected. The absence of sensitization by NO indicates that peroxide radicals were unimportant under the investigated conditions. A detailed chemical kinetic model for oxidation of acetonitrile was developed, based on a critical evaluation of data from literature. The rate coefficients for the reactions of CH_3CN and CH_2CN with O_2 were calculated from ab initio theory. Modeling predictions were in satisfactory agreement with experiments. Calculations were sensitive to the thermal dissociation of CH_3CN and to the branching fraction for $CH_3CN + OH$ to $CH_2CN + H_2O$ and $HOCN + CH_3$, respectively. More work is desirable for these steps, as well as for reactions of CH_2CN and HCCN.

Acknowledgements

The authors would like to thank John Mackie for helpful discussions. The authors acknowledge the financial support from MCIU-Spain (Project RTI2018-098856-B-100) and from Orient's Fund. Computational facilities were provided in part by National Science Foundation grant CHE-1531468.

References

References

[1] A. Doughty and J.C. Mackie. Kinetics of Thermal Decomposition of the Diazines: Shock-Tube Pyrolysis of Pyrimidine. *J. Chem. Soc. Faraday*, 90:541–548, 1994.

[2] A. Doughty, J.C. Mackie, and J.M. Palmer. Kinetics of the Thermal Decomposition and Isomerization of Pyrazine (1,4 Diazine). *Int. (Symp.) Combust.*, 25:893–900, 1994.

[3] A. Lifshitz, M. Bidani, A. Agranat, and A. Suslensky. Thermal Reactions of Pyrrolidine at Elevated Temperatures. Studies with a Single-Pulse Shock Tube. *J. Phys. Chem.*, 91:6043–6048, 1987.

[4] K.D. Bartle, J.M. Taylor, and A. Williams. Release of Nitrogen Compounds from Coal during High Temperature Pyroprobe Gas Chromatography with Selective Detection. *Fuel*, 71:714–715, 1992.

[5] P. Glarborg, M.U. Alzueta, K. Dam-Johansen, and J.A. Miller. Kinetic modeling of hydrocarbon/nitric oxide interactions in a flow reactor. *Combust. Flame*, 115:1–27, 1998.

[6] P. Glarborg, A.D. Jensen, and J.E. Johnsson. Fuel nitrogen conversion in solid fuel fired systems. *Prog. Energy Combust. Sci.*, 29:89–113, 2003.

[7] T. W. Asmus and T. J. Houser. Pyrolysis kinetics of acetonitrile. *J. Phys. Chem.*, 73:2555–2558, 1969.

[8] E. Metcalfe, D. Booth, H. McAndrew, and W.D. Wooley. The pyrolysis of organic nitriles. *Fire Mater.*, 7:185–192, 1983.

[9] A. Lifshitz, A. Moran, and S. Bidani. Thermal reactions of acetonitrile at high temperatures. Pyrolysis behind reflected shocks. *Int. J. Chem. Kin.*, 19:61–79, 1987.

[10] A. Lifshitz, M. Bidani, A. Suslensky, and C. Tamburu. Pyrolysis of Acrylonitrile at Elevated Temperatures. Studies with a Single-Pulse Shock Tube. *J. Phys. Chem.*, 93:1369–1373, 1989.

[11] E. Ikeda and J.C. Mackie. A kinetic study of the oxidation of acetonitrile: A model for NO formation from fuel-bound nitrogen. *Symp. (Int.) Combust.*, 26:597–604, 1996.

[12] A. Lifshitz, C. Tamburu, and H.F. Carroll. Thermal ignition of acetonitrile. Experimental results and kinetic modeling. *Int. J. Chem. Kin.*, 29:839–849, 1997.

[13] A. Lifshitz and C. Tamburu. Thermal Decomposition of Acetonitrile. Kinetic Modeling. *Int. J. Chem. Kinet.*, 30:341–347, 1998.

[14] K. Sendt, E. Ikeda, G.B. Bacskay, and J.C. Mackie. Ab initio quantum chemical and experimental (shock tube) studies of the pyrolysis kinetics of acetonitrile. *J. Phys. Chem. A*, 103:1054–1072, 1999.

[15] A.E. Axworthy. Chemistry and Kinetics of Fuel Nitrogen Conversion to Nitric Oxide. *AIChE Symp. Ser. 71*, 148:43–50, 1975.

[16] A.E. Axworthy, V.H. Dayan, and G.B. Martin. Reactions of Fuel-Nitrogen Compounds Under Conditions of Inert Pyrolysis. *Fuel*, 57:29–35, 1978.

[17] A. Lifshitz, Y. Cohen, M. Braun-Unkhoff, and P. Frank. Thermal Decomposition of Benzonitrile: A Combined Single Pulse Shock Tube–ARAS Investigation. *Proc. Combust. Inst.*, 26:659–667, 1996.

[18] T. Mendiara and P. Glarborg. Ammonia chemistry in oxy-fuel combustion of methane. *Combust. Flame*, 156:1937–1949, 2009.

[19] B. A. Williams and J. W. Fleming. Radical species profiles in low-pressure methane flames containing fuel nitrogen compounds. *Combust. Flame*, 110:1–97, 1997.

[20] J. C. Kramlich, J. A. Cole, J. M. McCarthy, W. S. Lanier, and J. A. McSorly. Mechanisms of nitrous-oxide formation in coal flames. *Combust. Flame*, 77:375–384, 1989.

[21] P. Glarborg, J.A. Miller, B. Ruscic, and S.J. Klippenstein. Modeling nitrogen chemistry in combustion. *Prog. Energy Combust. Sci.*, 67:31–68, 2018.

[22] M. U. Alzueta, P. Glarborg, and K. Dam-Johansen. Low temperature interactions between hydrocarbons and nitric oxide: An experimental study. *Combust. Flame*, 109:25–36, 1997.

[23] M. U. Alzueta, R. Bilbao, and M. Finestra. Methanol oxidation and its interaction with nitric oxide. *Energy Fuels*, 15:724–729, 2001.

[24] M. Abián, J. Giménez-López, R. Bilbao, and M.U. Alzueta. Effect of different concentration levels of CO_2 and H_2O on the oxidation of CO: Experiments and modeling. *Proc. Combust. Inst.*, 33:317–323, 2011.

[25] P.G. Kristensen, P. Glarborg, and K. Dam-Johansen. Nitrogen chemistry during burnout in fuel-staged combustion. *Combust. Flame*, 107:211–222, 1996.

[26] E. Goos, A. Burcat, and B. Ruscic. *Ideal gas thermochemical database with updates from Active Thermochemical Tables*. (<ftp://ftp. technion. ac. il/pub/supported/aetdd/thermodynamics> mirrored at <http://-garfield. chem. elte. hu/burcat/burcat. html>, 2016.

[27] B. Wang, H. Hou, and Y. Gu. Theoretical study of the reaction of atomic hydrogen with acetonitrile. *J. Phys. Chem. A*, 105:156–164, 2001.

[28] J. Sun, Y. Tang, X. Jia, F. Wang, H. Sun, J. Feng, X. Pan, L. Hao, and R. Wang. Theoretical study for the reaction of CH_3CN with O(3P). *J. Chem. Phys.*, 132:064301, 2010.

[29] Q.-S. Li and C. Y. Wang. Direct dynamic study on the hydrogen abstraction reaction $CH_3CN+OH \rightarrow CH_2CN+ H_2O$. *J. Comput. Chem.*, 25:251–257, 2004.

[30] C. Sleiman, S. González, S.J. Klippenstein, D. Talbi, G. El Dib, and A. Canosa. Pressure dependent low temperature kinetics for CN + CH_3CN: competition between chemical reaction and van der Waals complex formation. *Phys. Chem. Chem. Phys.*, 18:15118–15132, 2016.

[31] K. Hoyermann and J. Seeba. Mechanism and rate of the reaction of cyanomethyl radicals with oxygen atoms in the gas phase. *Z. Phys. Chem.*, 188:215–226, 1995.

[32] J. D. Adamson, J. D. DeSain, R. F. Curl, and G. P. Glass. Reaction of cyanomethylene with nitric oxide and oxygen at 298 K: HCCN + NO, O_2. *J. Phys. Chem. A*, 101:864–870, 1997.

[33] N.-Y. Chang and C.-H. Yu. Ab initio study of the dissociation of formyl cyanide. *Chem. Phys. Lett.*, 242:232–237, 1995.

[34] Y. Tang, R. Wang, and B. Wang. Theoretical study on mechanisms and kinetics of NCCO+O_2 reaction. *J. Phys. Chem. A*, 112:5295–5299, 2008.

[35] J. Troe. Predictive Possibilities of Unimolecular Rate Theory. *J. Phys. Chem.*, 83:114–128, 1979.

[36] C.J. Cobos and J. Troe. Prediction of Reduced Falloff Curves for Recombination Reactions at Low Temperatures. *Z. Phys. Chem.*, 217:1031–1044, 2003.

[37] A.J. Hynes and P.H. Wine. Kinetics and mechanism of the reaction of hydroxyl radicals with acetonitrile under atmospheric conditions. *J. Phys. Chem.*, 95:1232–1240, 1991.

[38] G. S. Tyndall, J. J. Orlando, T. J. Wallington, and M. D. Hurley. Products of the chlorine-atom- and hydroxyl-radical-initiated oxidation of CH_3CN. *J. Phys. Chem. A*, 105:5380–5384, 2001.

[39] A. Galano. Mechanism of OH radical reactions with HCN and CH_3CN: OH regeneration in the presence of O_2. *J. Phys. Chem. A*, 111:5086–5091, 2007.

[40] G. W. Harris, T. E. Kleindienst, and J. N. Pitts Jr. Rate constants for the reaction of OH radicals with CH_3CN, C_2H_5CN and CH_3CHCN in the temperature range 298–424 K. *Chem. Phys. Lett.*, 80:479–483, 1981.

[41] M. J. Kurylo and G. L. Knable. A kinetics investigation of the gas-phase reactions of Cl(2P) and OH(X2II) with CH_3CN: Atmospheric significance and evidence for decreased reactivity between strong electrophiles. *J. Phys. Chem.*, 88:3305–3308, 1984.

[42] G. Poulet, G. Laverdet, J.L. Jourdain, and G. Le Bras. Kinetic study of the reactions of acetonitrile with chlorine (Cl) and hydroxyl radicals. *J. Phys. Chem.*, 88:6259–6263, 1984.

[43] J. W. S. Jamieson, G. R. Brown, and J. S. Tanner. The reaction of atomic hydrogen with methyl cyanide. *Can. J. Chem.*, 48:3619–3622, 1970.

[44] R.J. Bonanno, R.B. Timmons, L.J. Stief, and R.B. Klemm. The kinetics and mechanisms of the reactions of O(3P) atoms with CH_3CN and CF_3CN. *J. Chem. Phys.*, 66:92–98, 1977.

[45] Y. Zhao and D.G. Truhlar. The M06 Suite of Density Functionals for Main Group Thermochemistry, Thermochemical Kinetics, Noncovalent Interactions, Excited States, and Transition Elements: Two New Func-

tionals and Systematic Testing of Four M06 Functionals and Twelve Other Functionals. *Theor. Chem. Acc.*, 120:215–241, 2008.

[46] I. M. Alecu, J. Zheng, Y. Zhao, and D. G. Truhlar. Computational Thermochemistry: Scale Factor Databases and Scale Factors for Vibrational Frequencies Obtained from Electronic Model Chemistries. *J. Chem. Theory Comput.*, 6:2872–2887, 2010.

[47] J. W. Ochterski, G. A. Petersson, and J. A. Montgomery Jr. A complete basis set model chemistry. V. Extensions to six or more heavy atoms. *J. Chem. Phys.*, 104:2598–2619, 1996.

[48] B. Ruscic. *Active Thermochemical Tables (ATcT) values based on ver. 1.118 of the Thermochemical Network*. (available at ATcT.anl.gov), 2015.

[49] P. Glarborg, C. S. Andreasen, H. Hashemi, R. Qian, and P. Marshall. Oxidation of methylamine. *in preparation*, 2020.

[50] M. J. Frisch et al. Gaussian 16. Technical Report Rev. A.03, Wallingford, CT, 2016.

[51] J. R. Barker et al. MultiWell-2019 Software Suite. Technical report, University of Michigan, Ann Arbor, MI, 2019, http://clasp-research.engin.umich.edu/multiwell/.

[52] A. Masaki, S. Tsunashima, and N. Washida. Rate constants for reactions of substituted methyl radicals (CH_2OCH_3, CH_2NH_2, CH_2I, and CH_2CN) with O_2. *J. Phys. Chem.*, 99:13126–13131, 1995.

[53] D.Q. Wang, H.L. Liu, X.R. Huang, Y. Li, C.Y. Geng, J.H. Zhan, and C.C. Sun. Diatomic radical-molecule reactions HCCN + O_2: mechanistic study. *European Phys. J. D*, 48:187–196, 2008.

[54] T. Imamura and N. Washida. Rate constants for the reactions of HCCCO and NCCO radicals with molecular oxygen. *Int. J. Chem. Kin.*, 33:440–448, 2001.

[55] W. Feng and J. F. Hershberger. Infrared diode laser study of the kinetics of the NCCO + O_2 reaction. *Chem. Phys. Lett.*, 488:140–144, 2010.

[56] W. Feng and J. F. Hershberger. Kinetics and Mechanism of the NCCO plus NO Reaction. *J. Phys. Chem. A*, 114:6843–6849, 2010.

[57] *ANSYS Chemkin PRO 2019 R3.* ANSYS, Inc., 2019.